Performance Evaluation and Delay-Power Trade-off Analysis of ZigBee Protocol

*Soumen Moulik, *Member*, *IEEE*, †Sudip Misra, *Senior Member*, *IEEE*, ‡Chandan Chakraborty
*Department of Computer Science and Engineering,
National Institute of Technology Meghalaya, Shillong - 793003, India.
†Department of Computer Science and Engineering, ‡School of Medical Science and Technology,
Indian Institute of Technology, Kharagpur - 721302, India.
Email: *smoulik@nitm.ac.in, †smisra@sit.iitkgp.ernet.in, ‡chandanc@smst.iitkgp.ernet.in

***Abstract*—In this paper, we analyze the superframe structure of the Medium Access Control (MAC) sublayer of IEEE 802.15.4 protocol (ZigBee), designed for Low-Rate Wireless Personal Area Networks (LR-WPANs), and evaluate the effects of the inactive portion of a superframe on average delay, and average power consumption. The four-dimensional Markov chain-based analysis of the slotted Carrier Sense Multiple Access with Collision Avoidance (CSMA/CA) algorithm presented in this work considers backoff freezing and acknowledged packet transmission that are not studied in the existing works. The analytical results prove that the performance of LR-WPANs depends significantly on the length of a superframe's active portion. We introduce a variable – Superframe duration-Beacon interval Ratio (SBR), which is utilized by tuning a few MAC parameters to achieve 35% reduced delay, on an average, compared to the existing state of the art. The results show that the proposed model also yields improved performance in terms of power consumption, for short and medium contention windows. In addition to the proposed analysis, this work provides optimized superframe order values that achieve trade-offs between delay and power consumption as demanded by user-provided QoS requirements corresponding to different contexts.**

***Index Terms*—Wireless Personal Area Networks, IEEE 802.15.4 Protocol, Zigbee, Slotted CSMA/CA, Superframe Duration, Beacon Interval, Trade-off, Tuning of MAC Parameters.**

I. Introduction

Two extensive efforts by the IEEE 802.15 working group revolutionized modern resource-constrained communication paradigm, which helped us to envision – *ubiquitous networking* [1] in our daily lives. Among them, the first is the development of IEEE 802.15.3a for high-rate WPANs, and another is the specification of ZigBee, i.e., the IEEE 802.15.4 protocol [2] for LR-WPANs. In this paper, we discuss the MAC sublayer of IEEE 802.15.4 protocol, and analyze average delay, average power consumption, and a trade-off between them in detail.

Most of the control and industrial applications appeal stringent QoS requirements such as real-time communication, low energy consumption, and reliable data delivery [3]. However, in many cases, the requirements are contradictory in nature such as simultaneous request to reduce delay and low energy consumption. Thus, the applications must come to a trade-off between the QoS attributes. This motivates us to perform a rigorous analysis of the slotted CSMA/CA algorithm – the beacon enabled channel access mechanism of IEEE 802.15.4 MAC layer, for identifying some of the key attributes that affect the delay and power consumption in a WPAN.

The contributions of the proposed work are as follows.

- We propose a Markov model-based analysis that pays attention to the existence of the inactive portion in a superframe and the backoff freezing mechanism. Acknowledgment (ACK) timeout is also considered in the proposed Markov model.
- A precise model of average delay and average power consumption in IEEE 802.15.4 MAC is proposed along with the analysis of impact of MAC parameters on them.
- We introduce a variable – Superframe duration-Beacon Interval Ratio (SBR) for adaptive tuning to achieve a trade-off between delay and power consumption.
- In addition to the constrained optimization of average delay and average power consumption, we also propose a generalized solution based on fuzzy inference, to achieve necessary trade-off.

II. Background

In case of beacon-enabled LR-WPANs, the PAN coordinator sends beacon frames in periodic intervals to synchronize network communication among the attached devices. Superframe is the channel time that is bounded by two consecutive beacon frames, as illustrated in Figure 1. Superframes are subdivided into an *active period* and an *inactive period* [2]. During the inactive period, sensor devices may switch off their transceivers and go into sleep state. Transceivers communicate in the active period, which again is partitioned into two parts – a Contention Access Period (CAP) and a Contention Free Period (CFP). The CAP starts immediately after the beacon frame transmission and ends at the beginning of the CFP on a superframe slot boundary. The transmission within the CAP period strictly follows the slotted CSMA/CA algorithm to access the channel. On the contrary, no transmission is allowed to follow this algorithm within CFP, as the PAN coordinator allocates Guaranteed Time Slots (GTSs) for the devices from this period. The length of the active period is known as Superframe Duration (SD) and the time period

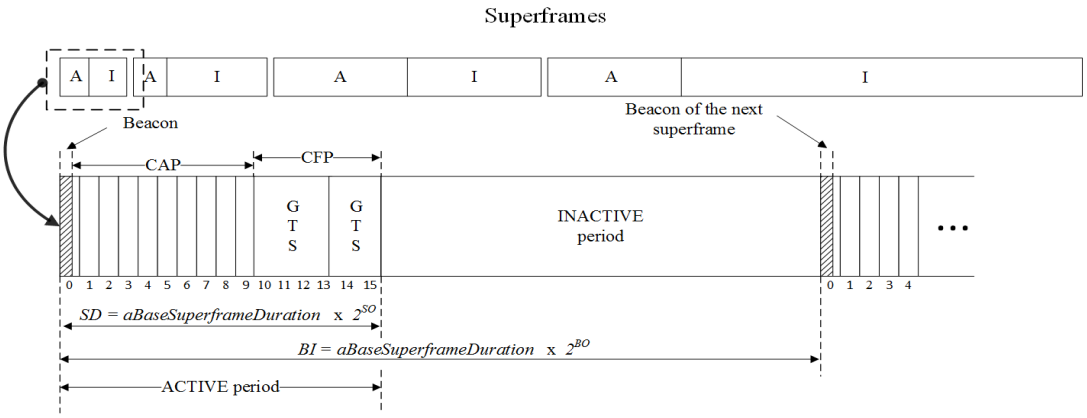

Fig. 1: Superframe structure in IEEE 802.15.4 protocol [2]

between two consecutive beacons is known as Beacon Interval (BI). The MAC maintains a Personal area network Information Base (PIB), where different attributes are stored with default values. Superframe Order (SO) and Beacon Order (BO) are two such attributes that control the length of SD and BI, respectively. The control relationships are explained in [2], and also illustrated in Figure 1. A significant amount of trade-off between delay and power consumption can be achieved by modifying the lengths of SD and BI, i.e., by tuning the values of SO and BO.

A brief description of the slotted CSMA/CA algorithm [2] is also required for better understanding of the proposed model. The three important attributes related to this algorithm are – number of backoffs (NB), congestion window (CW) size, and backoff exponent (BE). The time slots making up the CAP are subdivided into smaller time slots known as backoff periods. One backoff period generally has a default length corresponding to 20 channel symbols times. Before the successful transmission of a packet, each node must wait a random number of backoff periods followed by two Clear Channel Assessments (CCAs). The random number of backoff periods is selected between 0 and $(2^{BE} - 1)$. The MAC PIB attribute *macMinBE* stores the minimum value of BE, and according to CSMA algorithm BE is initialized with this value. The value of CW is initialized with 2, as channel sensing or the CCA is performed twice. The value of CW is decremented by 1 after each CCA, and a packet is transmitted only if the current value of CW is 0. The value of NB is initialized with 0. If the channel is sensed as busy in any of the CCA then NB is incremented by 1, and the node again repeats the steps from waiting for random backoff periods. However, a maximum limit of NB does exist, and the PIB attribute *macMaxCSMABackoffs* stores this maximum allowable value of NB. The current packet transmission is considered as failed if NB exceeds this maximum value. However, in the proposed model we exploit another MAC PIB attribute *macMaxFrameRetries*, which stores the number of maximum allowable re-transmission attempts. Apart from the NB value exceeding its maximum limit, a packet transmission may be discarded due to consecutive ACK timeouts. Whenever an ACK timeout occurs in any backoff stage, the packet transmission does not get discarded. Rather, re-transmission of the packet takes place, until the re-transmission counter reaches its maximum value stored in *macMaxFrameRetries*.

The reason that leads to the case of discarding a packet is exceeding this retry limit due to successive channel failures, or ACK timeouts. A successful channel sense does not always guarantee a successful packet delivery at the destination. In between the source and the destination, the packet may collide, or even in case of successful delivery of the packet, the ACK packet from the destination may collide in its path, leading to an ACK timeout. However, consecutive ACK timeouts or channel failures may lead to a re-transmission counter value higher than the *macMaxFrameRetries*, and the packet is considered as discarded in such cases.

III. Related Works

We categorize the existing works on performance analysis of the ZigBee protocol in different groups and discuss them. In simulation-based analysis, the works [4]–[7] are significant. In one of the earliest works in this domain, Lu et al. [4] proposed simulation-based performance evaluation for a star topology in a beacon-enabled mode. The authors evaluated energy consumption, latency, throughput, and packet delivery ratio in both the cases of 100% and less than 100% duty cycle. Bougard et al. [5] presented the energy consumption breakdown among the different phases of packet transmission. Koubaa et al. [6] simulated the performance of slotted CSMA/CA for different network settings to analyze the impact of protocol attributes, such as SO, BO, and BE on network performance. Zheng and Lee [7] further studied several other issues such as association through tree formation, coordinator relocation, and guaranteed time-slot allocation in their simulation-based study. However, these works are limited due to the lack of a concrete model which is able to optimize different MAC attributes considered in the PIB, in order to meet the required QoS demands. These works are based on specific scenarios, and they lack the effect of variable inactive period length. The work described in [6] focuses only on the BO without considering the repercussion of SO on network performance. Thus, in the proposed work, we address these limitations by modeling the slotted CSMA/CA algorithm with a four-dimensional Markov chain.

Inspired by Bianchi's Markov-chain based analysis for IEEE 802.11 DCF [8], different authors developed analytical models for the slotted CSMA/CA mechanism. Misic et al. [9] used the discrete time Markov chains and $M/G/1/K$ queues in order to implement packet transmission in non-saturation mode. Further, the authors expanded this work for downlink traffic and acknowledged transmission in [10]. Ling et al. [11] modeled the slotted CSMA/CA mechanism with three-level renewal process, and evaluated throughput and service time for both saturated and unsaturated traffic conditions. However, as these works used the concepts of queuing theory and renewal process, numerical methods were used extensively to solve nonlinear equations, which is a major limitation from computational perspective in LR-WPANs.

Using a Markov model-based approach, Sahoo and Sheu [12] derived an analytical model for the slotted CSMA/CA with considering the packet retry limits. Pollin et al. [13] provided a detailed analytical evaluation for both uplink and acknowledged traffic, based on a two-dimensional Markov chain in a star topology network. The authors also performed the analysis of throughput and the energy consumption for some specific ranges. Jung et al. [14] proposed a Markov model for unsaturated traffic conditions, considering super-frame structure, acknowledged transmission, and retransmission with and without limit. In a similar way, Buratti et al. [15] and Faridi et al. [16] also proposed their respective models for slotted CSMA/CA. However, these models are unable to holistically capture the functionality of this algorithm.

Various algorithms were proposed to tune the MAC parameters of the IEEE 802.15.4 protocol. Misic et al. [17] addressed the trade-off between the desired data rate and the lifetime of individual sensors using analytical modeling of network reliability in beacon-enabled mode. Again, the use of $M/G/1/K$ queues made this work computationally extensive. Moreover, the algorithm discussed in this may require modifications of the standard. Park et al. [18], [19] proposed adaptive tuning of MAC parameters in order to achieve energy-efficient, reliable, and timely communication. The authors used three-dimensional Markov chain to model the slotted CSMA/CA in their works. Markov chain-based approach is also taken in the work proposed by Moulik et al. [20], where the authors optimized the MAC-frame payload to achieve maximized transmission reliability.

Synthesis: The existing Markov chain analyses of the slotted CSMA/CA protocol [12]–[20], and the other non-Markov works [21]–[23] primarily do not consider the existence of this inactive portion, and thus, are based on an assumption of not considering the backoff freezing event in their Markov model. Moreover, except [19] all other works do not involve the important event of ACK timeout in their model. Most of the existing works overlooked the fact that PIB attributes like SO and BO have significant effects on QoS attributes such as – delay and the power consumption. Even if few of them [4], [6] realized it, the lack of proper model and optimization approach to meet rigorous QoS requirements is felt. The proposed Markov chain-based analysis addresses these assumptions and limitations, and paves the path of a trade-off between delay and power consumption. Moreover, optimal values of SO and corresponding SBRs are derived with the help of MATLAB's genetic algorithm-based constrained minimization method and fuzzy inference. Section V and VI discuss the results in detail.

TABLE I: Different parameters used and their values

Param.	Value	Description
m_0	$0-2$	*macMinBE*: minimum value of BE
m	$2-5$	*macMaxCSMABackoffs*: maximum number of CSMA backoff stages
W_i	$2^i W_0$, where $W_0 = 2^{m_0}$	maximum number of backoff periods for i^{th} backoff stage
r	3	*macMaxFrameRetries*: maximum retry limit
L_b	120	*macAckWaitDuration*: ACK timeout duration in symbol periods
$s(t)$	-1	Event of discarding a packet after exceeding the maximum retry limit
	i, where $i \in [0, m]$	All events starting from random wait to ACK timeout, in i^{th} backoff stage
$c(t)$	j, where $j \in [0, W_i - 1]$	Backoff decrements while waiting for random backoff periods before the first CCA, in i^{th} backoff stage
	-1	First CCA
	-2	Second CCA
	-3	Event of transmitting a packet and receiving corresponding ACK or facing ACK timeout
$n(t)$	k, where $k \in [0, r]$	k^{th} re-transmission attempt
$a(t)$	0	Events that belongs to the active period of a superframe
	-1	Events that belongs to the inactive period of a superframe
	-2	Packet delivered successfully and ACK is received withing timeout
	l, where $l \in [1, L_b]$	Time slots representing the packet transmission and the wait for ACK

In order to address these lacunae we consider the distinction of the active and the inactive portions by introducing a dedicated tuple in the proposed Markov chain. Using this tuple we also manage the waiting duration, due to packet transmission and ACK reception, until the ACK timeout occurs. We denote γ as the probability of not receiving an ACK, and consider this in the chain until the ACK timeout, which is signified by L_b slots. The minimum number of slots that the source has to wait before expecting an ACK from the receiver is considered as L_a. In order to identify the inactive portion in the Markov chain, we consider a variable P_{W_i-1}, i.e., the probability of finding the CAP end in a backoff slot boundary in the i^{th} backoff stage of each retry attempt. We incorporate the backoff freezing mechanism by considering the variable λ_s, which represents the probability of not finding the end of the inactive portion, viz., the probability of not finding the *beacon* of the next superframe. Moreover, we introduce a variable SBR, as the ratio of SD to BI, and discuss the significance of this variable in result section.

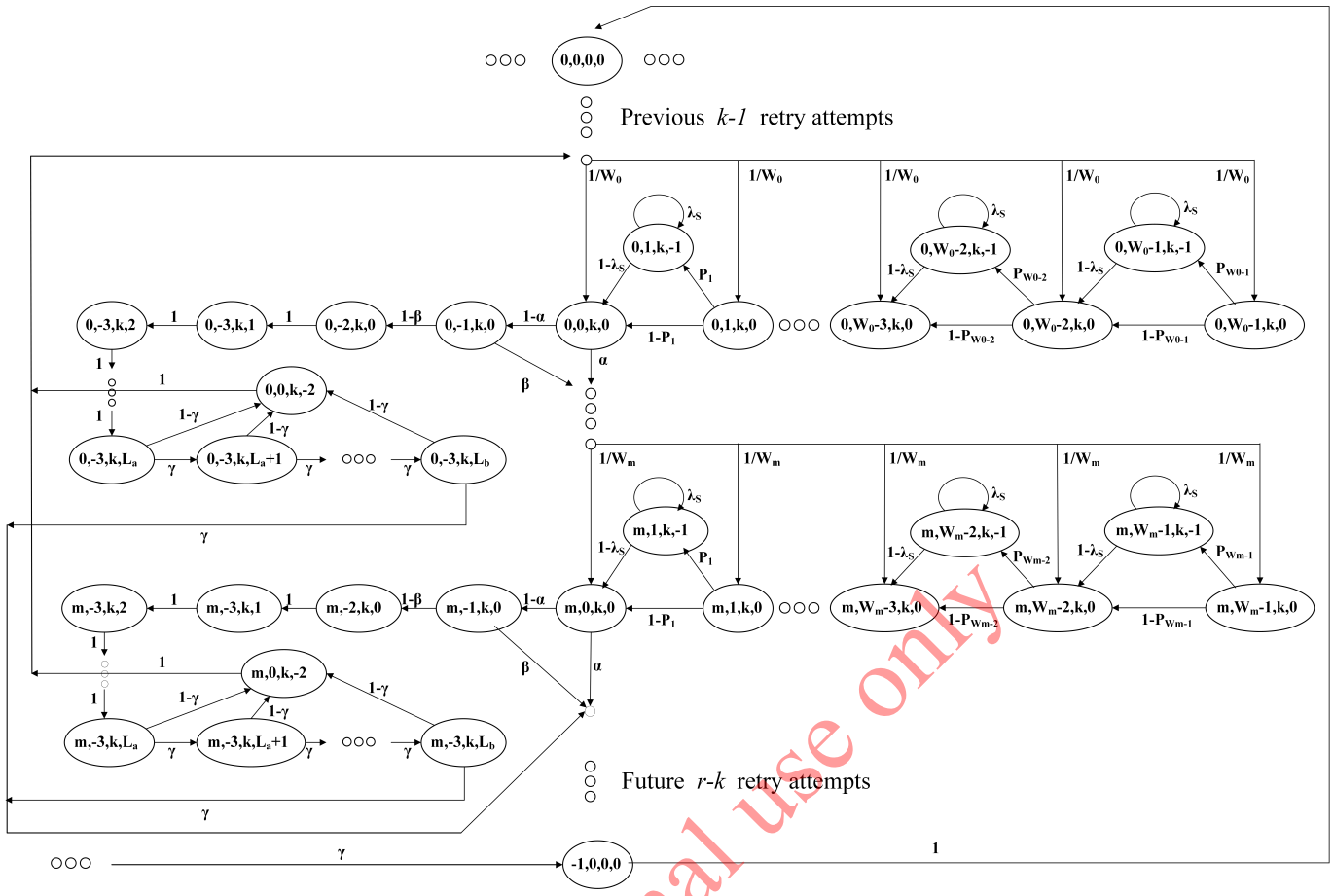

Fig. 2: Proposed Markov chain-based model for IEEE 802.15.4

IV. Proposed Analytical Model for IEEE 802.15.4

In this section, we propose a Markov chain model of the slotted CSMA/CA algorithm, while considering the existence of inactive portion in a superframe, retry limits, and acknowledged transmission. We break the slotted CSMA/CA algorithm into different distinguishable parts, and derive the expressions for each part. We also prove the validity of the proposed model. We assume that $s(t)$, $c(t)$, $n(t)$, and $a(t)$ are the stochastic processes that represent the backoff stage, the slot-position of the backoff counter, the value of retransmission counter, and the state of the node, i.e., whether it is in the active state, or the inactive state, in transmitting phase, or in the ACK-receiving phase within the ACK timeout, at time t respectively, as illustrated in Figure 2. The quadruple ($s(t)$, $c(t)$, $n(t)$, $a(t)$) represents the four-dimensional Markov chain proposed in this work. However, due to the complexity of the full Markov chain, Figure 2 only illustrates the structure of the k^{th} retry attempt. We denote the MAC parameters considered in this work by $W_0 \leftarrow 2^{macMinBE}$, $m \leftarrow macMaxCSMABackoffs$, and $r \leftarrow macMaxFrameRetries$. A detailed list of different parameters, their values and meanings are summarized in Table I.

The single state $(-1, 0, 0, 0)$ solely represents the event of discarding a packet due to the channel access failure in the last backoff stage in last retry attempt, or due to the lack of ACK reception within ACK timeout. The states from $(i, W_i - 1, k, 0)$ to $(i, 0, k, 0)$ represent the backoff decrement inside the active portion of the superframe, at i^{th} backoff stage, in k^{th} retry limit. On the contrary, the states from $(i, W_i - 1, k, -1)$ to $(i, 0, k, -1)$ infer the possibilities of backoff freezing at i^{th} backoff stage, in k^{th} retry limit, in case the current backoff slot boundary represent the start of the inactive portion of the superframe. In a similar manner, the states $(i, -1, k, 0)$ and $(i, -2, k, 0)$ represent first and second CCA, respectively. As illustrated in Figure 2, the probabilities of getting the channel busy during first and second CCA are α and β, respectively. The states $(i, 0, k, -2)$ represent ACK reception within ACK timeout. Again, the states from $(i, -3, k, 1)$ to $(i, -3, k, L_b)$ represent the packet transmission and the corresponding ACK reception phases till the ACK timeout in slotted format. Therefore, as per our consideration, the stochastic process $a(t)$ is 0 when the node is in the active portion, -1 when the node is in inactive state, -2 in case of successful packet delivery, and otherwise, any value among 1 to L_b. Thus, the consideration of this new stochastic process $a(t)$ is very effective in order to analyze the Markov chain regularities more accurately than the existing works that follow a similar approach. The state transition probabilities associated with the proposed Markov model are derived as follows:

$$P\{(i,0,k,0) \mid (i-1,0,k,0)\} = \alpha + (1-\alpha)\beta \quad \text{for } i \in [1,m],\ k \in [0,r]. \tag{1}$$

$$P\{(i,j,k,-1) \mid (i,j,k,0)\} = P_j \quad \text{for } i \in [0,m],\ j \in [1,W_i-1],\ k \in [0,r]. \tag{2}$$

$$P\{(i,j,k,-1) \mid (i,j,k,-1)\} = \lambda_s \quad \text{for } i \in [0,m],\ j \in [1,W_i-1],\ k \in [0,r]. \tag{3}$$

$$P\{(i,j-1,k,0) \mid (i,j,k,-1)\} = 1-\lambda_s \quad \text{for } i \in [0,m],\ j \in [1,W_i-1],\ k \in [0,r]. \tag{4}$$

$$P\{(i,j-1,k,0) \mid (i,j,k,0)\} = 1-P_j \quad \text{for } i \in [0,m],\ j \in [1,W_i-1],\ k \in [0,r]. \tag{5}$$

$$P\{(i,-1,k,0) \mid (i,0,k,0)\} = 1-\alpha \quad \text{for } i \in [0,m], k \in [0,r]. \tag{6}$$

$$P\{(i,-2,k,0) \mid (i,-1,k,0)\} = 1-\beta \quad \text{for } i \in [0,m],\ k \in [0,r]. \tag{7}$$

$$P\{(i,-3,k,l) \mid (i,-3,k,l-1)\} = 1 \quad \text{for } i \in [0,m],\ k \in [0,r],\ l \in [1,L_a]. \tag{8}$$

$$P\{(i,-3,k,l) \mid (i,-3,k,l-1)\} = \gamma \quad \text{for } i \in [0,m],\ k \in [0,r],\ l \in [L_a+1,L_b]. \tag{9}$$

$$P\{(i,0,k,-2) \mid (i,-3,k,l)\} = 1-\gamma \quad \text{for } i \in [0,m],\ k \in [0,r],\ l \in [L_a,L_b]. \tag{10}$$

$$P\{(0,0,k,0) \mid (i,-3,k-1,L_b)\} = \gamma \quad \text{for } i \in [0,m],\ k \in [0,r]. \tag{11}$$

$$P\{(-1,0,0,0) \mid (i,-3,r,L_b)\} = \gamma \quad \text{for } i \in [0,m]. \tag{12}$$

$$P\{(0,0,0,0) \mid (i,0,k,-2)\} = 1 \quad \text{for } i \in [0,m],\ k \in [0,r]. \tag{13}$$

$$P\{(0,0,0,0) \mid (-1,0,0,0)\} = 1. \tag{14}$$

Equations (1) to (3) represent the increment of backoff stage in each retry limit, the transition between the active state and the inactive states, and the waiting time in the inactive state, viz. the backoff freezing, resepectively. Equation (4) represents the transition from the inactive state of the current superframe to the active state of the next supeframe. The effective transition probability from one backoff counter to another backoff counter is illustrated in Equation (5). Equations (6) to (9) represent the first CCA, the second CCA, the packet transmission, and the waiting for acknowledgment from the receiver, respectively. Equations (10) and (11) represent successful packet transmission, and ACK timeout, respectively. Equation (12) represents the unsuccessful packet transmission in the last backoff stage in the last retry attempt, and the proceeding towards the next transmission attempt by resetting the values of W_0 and m. Equation (13) represents the consideration of a fresh transmission of a new packet, after the successful transmission of the current packet. Equation (14) represents that the system discards the current packet, and attempts the transmission of the next packet following the similar method. Among the other variables considered in this work, α and β represent the probability of finding the channel busy after first and second CCA, respectively. For the ease of approximation, we assume, P_{W_i-1} values for each stage, i.e., the probabilities of finding the CAP-end in a backoff slot boundary are equal after each backoff period, and consider each of them as P while deducing the expressions associated with the different parts of the slotted CSMA/CA algorithm.

Let $b_{i,j,k,l} = \lim_{t\to\infty} \hat{P}\big(s(t) = i,\ c(t) = j,\ n(t) = k,\ a(t) = l\big)$, where $i \in [-1,m]$, $j \in [-3,W_i-1]$, $k \in [0,r]$, and $l \in [-1,L_b]$ be the stationary distribution of the proposed Markov chain, and L_b is time duration that represents ACK timeout. The MAC PIB attribute $maxAckWaitDuration$ stores the value of L_b. Based on the chain regularities expressed in Equations (1) to (14), and the normalization condition, we know that

$$\sum_{i=0}^{m}\sum_{j=0}^{W_i}\sum_{k=0}^{r} b_{i,j,k,0} + \sum_{i=0}^{m}\sum_{j=0}^{W_i-1}\sum_{k=0}^{r} b_{i,j,k,-1} \quad + \sum_{i=0}^{m}\sum_{k=0}^{r} b_{i,-1,k,0} + \sum_{i=0}^{m}\sum_{k=0}^{r} b_{i,-2,k,0} \quad + \sum_{i=0}^{m}\sum_{k=0}^{r}\sum_{l=1}^{L_b} b_{i,-3,k,l} + \sum_{i=0}^{m}\sum_{k=0}^{r} b_{i,0,k,-2} + b_{-1,0,0,0} = 1 \tag{15}$$

Equation (15) represents the summation of different components of the slotted CSMA/CA mechanism in its left hand side. The components are – backoff decrement in active portion, backoff freze in inactive portion, first CCA, second CCA, transmissting and ACK receiving, successful reception of a packet, and discarding a packet, respectively. We derive the expressions of each component in the left hand side of Equation 15, in terms of $b_{0,0,0,0}$. The backoff decrement in the active portion, and the backoff freezing in the inactive portion, throughout all the backoff stages in all the retry attempts, is derived in terms of $b_{0,0,0,0}$, respectively, as follows:

$$\sum_{i=0}^{m}\sum_{j=0}^{W_i-1}\sum_{k=0}^{r} b_{i,j,k,0} = \frac{1}{2}\left[W_0\left(\frac{1-(2x)^{m+1}}{1-2x}\right) + \frac{1-x^{m+1}}{1-x}\right] \Psi\ b_{0,0,0,0} \tag{16}$$

$$\sum_{i=0}^{m}\sum_{j=0}^{W_i-1}\sum_{k=0}^{r} b_{i,j,k,-1} = \frac{P}{2(1-\lambda_s)}\left[W_0\left(\frac{1-(2x)^{m+1}}{1-2x}\right) - \frac{1-x^{m+1}}{1-x}\right] \Psi\ b_{0,0,0,0} \tag{17}$$

In a similar manner, the first CCA, second CCA, transmissting and ACK receiving, successful reception of a packet, and discarding a packet, are expressed respectively, as follows:

$$\sum_{i=0}^{m}\sum_{k=0}^{r} b_{i,-1,k,0} = (1-\alpha)\frac{1-x^{m+1}}{1-x}\ \Psi\ b_{0,0,0,0} \tag{18}$$

$$\sum_{i=0}^{m}\sum_{k=0}^{r} b_{i,-2,k,0} = (1-x^{m+1})\ \Psi\ b_{0,0,0,0} \tag{19}$$

$$\sum_{i=0}^{m}\sum_{k=0}^{r}\sum_{l=1}^{L_b} b_{i,-3,k,l} = (1-x^{m+1})\gamma^{L_b-L_a}\ \Psi\ b_{0,0,0,0} \tag{20}$$

$$\sum_{i=0}^{m}\sum_{k=0}^{r} b_{i,0,k,-2} = (1-\gamma^{L_b-L_a+1})(1-x^{m+1})\ \Psi\ b_{0,0,0,0} \tag{21}$$

$$b_{-1,0,0,0} = \left(\left[1-x^{m+1}\right]^{r+1}\gamma^{L_b-L_a+1} + x^{m+1}\right) b_{0,0,0,0} \tag{22}$$

where,
$$x = \alpha + (1-\alpha)\ \beta \tag{23}$$

$$\Psi = \frac{1-\left[\gamma^{L_b-L_a+1}\ (1-x^{m+1})\right]^{r+1}}{1-\gamma^{L_b-L_a+1}\ (1-x^{m+1})} \tag{24}$$

Equations (16) to (22) represent the state values $b_{i,j,k,l}$ as a function of $b_{0,0,0,0}$. We now replace the corresponding values in the normalization condition provided by Equation (15), in order to get the expression and value of $b_{0,0,0,0}$.

V. Analytical Results

In this section, we discuss few results based on our proposed analysis of the IEEE 802.15.4 protocol. We compare the obtained result with the recent work of Park et al. [19], and also discuss the significant achievements from the analysis.

A. Analysis of Delay

We consider the average delay for a successfully received packet as the time interval from the instant the packet inside the source buffer is considered for a transmission, until an ACK for the corresponding packet is received at the source. The packet dropping instances are not covered in this delay estimation. We replace the term $\frac{P}{1-\lambda_s}$ in Equation (17), with $\frac{BI-SD}{SD}$. The intuition behind this is, $(BI-SD)$ and SD represent the inactive portion and the active portion of the superframe, respectively. The probability of finding a CAP-end, i.e., the probability of finding the inactive portion in absence of CFP is represented by P. Again, $(1-\lambda_s)$ represents the probability of finding the end of an inactive portion, i.e., the probability of finding the active portion of the next superframe, in order to resume any ongoing transmission. Therefore, the expression $\frac{P}{1-\lambda_s}$ can be replaced with the expression $\frac{BI-SD}{SD}$. We only consider the delay for successful data delivery. Along with successful delivery (i.e., receiving the ACK within timeout) within a superframe, we also consider the scenario that requires multiple superframes. Thus, we also incorporate the backoff freezing scenario in our average delay calculation. Therefore, by adding Eq. (17) and Eq. (21) we derive the expression of average delay (D_{avg}) as follows:

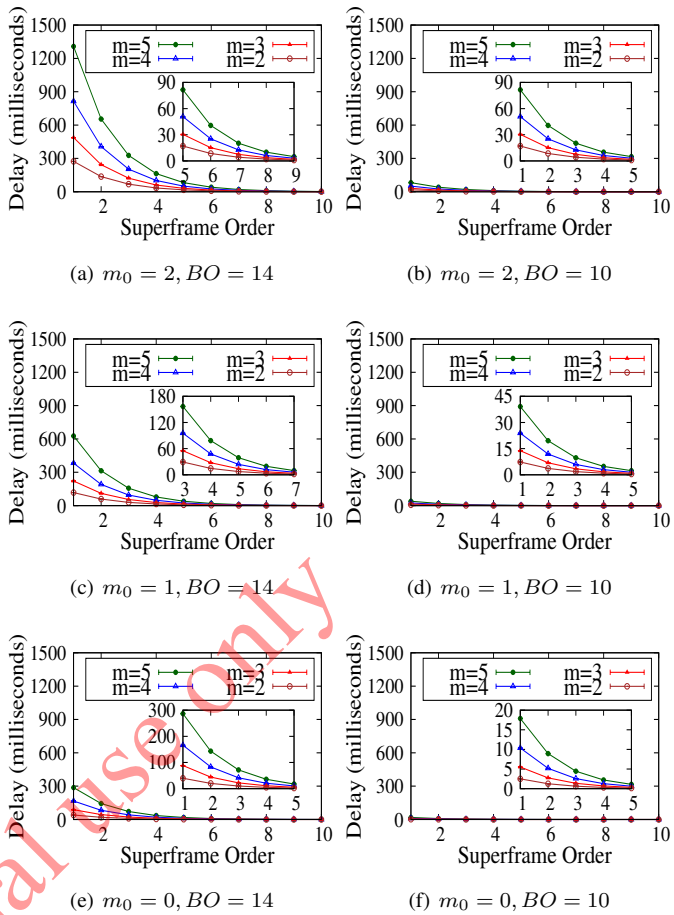

(a) $m_0 = 2, BO = 14$ (b) $m_0 = 2, BO = 10$

(c) $m_0 = 1, BO = 14$ (d) $m_0 = 1, BO = 10$

(e) $m_0 = 0, BO = 14$ (f) $m_0 = 0, BO = 10$

Fig. 3: Delay vs. Superframe Order with $BO = \{14, 10\}$ and $m_0 = \{2, 1, 0\}$

$$D_{avg} = \left(\frac{BI-SD}{2\ SD}\left[W_0\left(\frac{1-(2x)^{m+1}}{1-2x}\right) - \frac{1-x^{m+1}}{1-x}\right] + (1-\gamma^{L_b-L_a+1})\ (1-x^{m+1})\right)\ \Psi\ b_{0,0,0,0} \tag{25}$$

In case of slotted CSMA/CA, the source commences packet transmission at a backoff period boundary and the minimum time duartion to complete two CCAs, frame transmission, and ACK reception is considered as $aMinLIFSPeriod$. The source waits for the ACK until the ACK timeout, which is considered as $macAckWaitDuration$. In our analysis, we incorporate these time intervals through the variables L_a and L_b, respectively. The values of different parameters considered in these analyses are summarized in Table II.

Inference: Figure 3 illustrates the effects of SO on average delay in completing a full acknowledged packet transmission. We consider two different scenarios having different Beacon Intervals. The corresponding BOs are 14 and 10. We vary the parameter m_0, viz. the minimum backoff exponent, which is responsible to initialize the contention window size, and obtain results depicted in Figures 3(a) to 3(f). It is evident from the superframe structure described in Figure 1 that the length of the inactive portion reduces if the MAC layer considers

TABLE II: Different parameters used and their values

Parameters	Values
Data rate	250 bps
Base Slot Duration	60 symbol periods
$aMinLIFSPeriod$	40 symbol periods
$macAckWaitDuration$	120 symbol periods
Power consumption during packet transmission, packet reception, sleep, CCA, and idle	30 mW, 40 mW, 0.16 μW, 40 mW, 0.8 mW (respectively)

a high SD, keeping the BI unchanged, representing a high SBR. A high SD refers to a high expected probability of finding a CAP-end, at a random backoff slot, leveraging high chances to complete a packet transmission within the CAP-end of the current superframe. Evidently, the average delay is low in such cases. On the contrary, low SD reduces the length of the CAP, and thus, increases the chance of backoff-freezing in the inactive portion. It forces the source to continue the transmission in a new CAP in the next superframe, and thus, increases the average delay for a packet transmission. In addition, higher values of m_0 increases the chance of selecting a random backoff within a larger range, thus, may forces the source to face a backoff countdown of longer duration. The similar scenario occurs in case of large m, and seemingly both of these cases lead to high delay.

Another significant observation is the gradual convergence of the average delay for different m values, with the increase of SD. It may be inferred from this observation that small values of SD shortens the length of CAP, and thus, makes it difficult to complete a packet transmission before the beginning of the inactive portion. Therefore, very small SBR values involve multiple superframes while transmitting a single packet. In such cases, it is difficult to find the channel idle after the random backoff countdown, as the source frequently enters the inactive portion, and spend relatively more time there. Failures in channel sensing extends the contention window size, and forces the source to enter the next backoff stage, as described in Figure 2. Thus, the significance of m is much more in case of shorter SD, viz. low SBR. Consequently, the effect of m, for a particular m_0, fades away with the increase of SD, or with high SBR.

B. Analysis of Power Consumption

According to the proposed Markov chain, as illustrated in Figure 2, we break up the average power consumption (E_{tot}) into different phases. The average power consumption is represented as follows:

$$P_{avg} = P_{cs}\left(\sum_{i=0}^{m}\sum_{k=0}^{r} b_{i,-1,k,0} + \sum_{i=0}^{m}\sum_{k=0}^{r} b_{i,-2,k,0}\right) + P_i \sum_{i=0}^{m}\sum_{j=0}^{W_i-1}\sum_{k=0}^{r} b_{i,j,k,0} + P_s \sum_{i=0}^{m}\sum_{j=0}^{W_i-1}\sum_{k=0}^{r} b_{i,j,k,-1} + \left(P_{tx}+P_{rx}\right)\sum_{i=0}^{m}\sum_{k=0}^{r}\sum_{l=1}^{L_b} b_{i,-3,k,l} \quad (26)$$

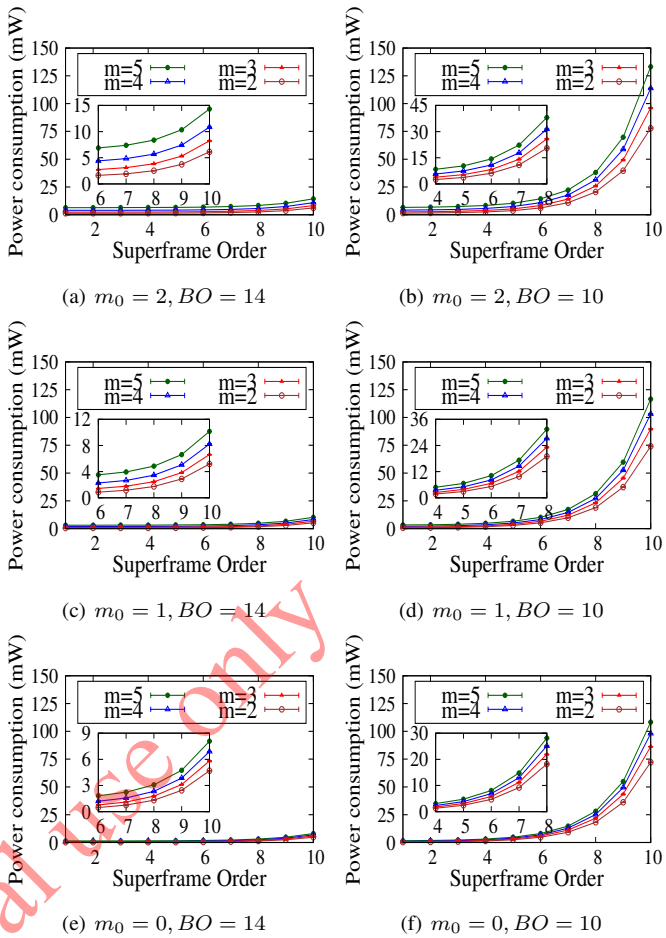

(a) $m_0 = 2, BO = 14$ (b) $m_0 = 2, BO = 10$

(c) $m_0 = 1, BO = 14$ (d) $m_0 = 1, BO = 10$

(e) $m_0 = 0, BO = 14$ (f) $m_0 = 0, BO = 10$

Fig. 4: Power consumption vs. Superframe Order with $BO = \{14, 10\}$ and $m_0 = \{2, 1, 0\}$

where, P_{cs}, P_i, P_s, P_{tx}, P_{rx} are the power consumption values during channel sensing, idle time, sleep mode, packet transmission, and ACK reception, respectively.

Inference: Figure 4 depicts the influence of SO on the average power consumption of a sensor device that operates under IEEE 802.15.4 protocol. Figures 4(a) to 4(f) further illustrate the analyses of power consumption for different m_0. According to our analysis, short SD leads to long inactive portion, or low SBR, for a fixed BI. Thus, inside a superframe, a packet mostly spends time in the inactive portion – a low-power-consuming state. In addition, short SD sometimes may influence the MAC layer to choose a random backoff within a short range, which indicates low power consumption during backoff countdown. Before the backoff countdown MAC layer always attempts to check whether the full transaction, i.e., the backoff decrement, two CCAs, frame transmission, and ACK reception can be completed in the current CAP or not, even if the number of randomly chosen backoffs are less than the available backoff slots in the CAP. On the contrary, higher SD, or low SBR is responsible for high power consumption. Moreover, the effect of m and m_0 over power consumption is negligible. However, m possess comparatively more influence than the m_0 as the high value of m is responsible for provisioning more channel sensing opportunities, after consecutive

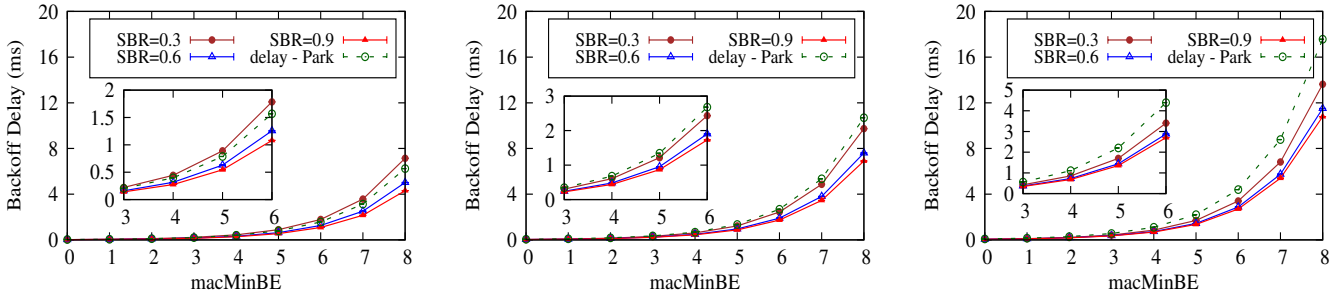

(a) $macMaxCSMABackoffs\ (m) = 3$ (b) $macMaxCSMABackoffs\ (m) = 4$ (c) $macMaxCSMABackoffs\ (m) = 5$

Fig. 5: Backoff Delay vs. MAC parameter $macMinBE$, for r=3

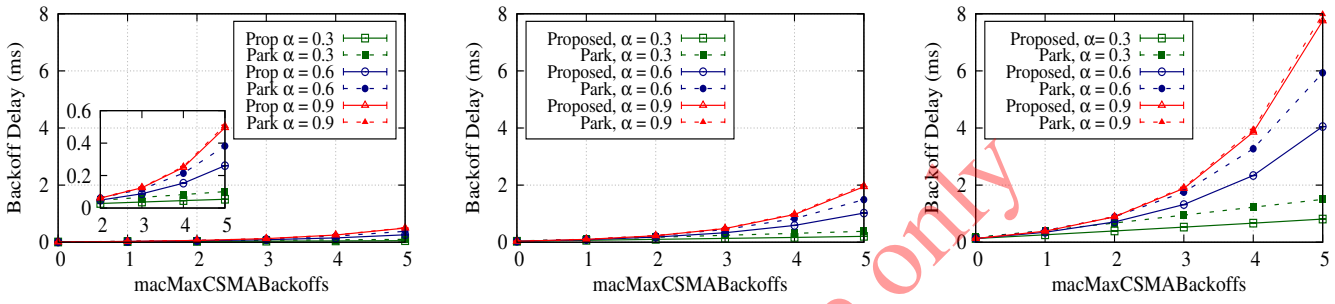

(a) $macMinBE(m_0) = 2$ (b) $macMinBE(m_0) = 4$ (c) $macMinBE(m_0) = 6$

Fig. 6: Backoff Delay vs. MAC parameter $macMaxCSMABackoffs$, for r=3

failures of the same.

C. Performance Comparison

In this subsection, we discuss the performance comparison between the proposed analysis and the analysis done by Park et al. [19]. We consider the average delay during backoff countdown in this comparison. In addition, we also compare the average power consumption, and observe that according to the proposed Markov chain the system consumes low power in most of the cases, except extremely high m_0 and m. Except the consideration of different values for m_0 and m, we consider same parameter values in the comparison.

Figures 5 and 6 compare the delay performance of the proposed model with the Park's model, for different m and m_0, respectively. The average backoff delay increases with the increase of m_0, and the rate of increase is directly proportional to the value of m, as depicted in Figure 5. Both the proposed analysis and Park's analysis follow this general trend of slotted CSMA/CA. However, the ratio SBR, considered explicitly in this analysis makes the difference, and clearly shows the achievements. From figures 5(a) to 5(c), it is evident that the average delay decreases with the consideration of high SBR values. The default value of m is 4, according to the IEEE 802.15.4 protocol standard [2]. We note from Figure 5(b) that the average delay of Park's model approximately overlaps with the proposed analysis, when the ratio SBR is considered as 0.3. For higher values of SBR, obviously the backoff delay is much less than the Park's model, achieving around 35% improvement in delay. Higher the value of m, the positive difference between the average delay of Park's model and the proposed model increases. From Figure 5(a), we note that the delay using our model is higher than that using Park's model, in case of $SBR = 0.3$. Therefore, in this case it is always possible to achieve better performance than the Park's model, if the concerned application tunes the variable SBR above 0.4, by choosing suitable SO and BO values.

In Figure 6, one obvious observation is the increase in backoff delay with the increase in m. The rate of increase is higher in case of higher m_0 values. Moreover, another important observation from Figures 6(a) to 6(c) is that the probability of a channel being busy has a significance in this comparison. We consider α and β to be equal, and observe that the proposed model achieves much reduced delay than the Park's model. However, for extremely high probability of busy channel, such as 0.9 and above, the backoff delay is approximately the same for both of these models.

Figures 7 and 8 compare the power consumption of the proposed model with the model derived by Park et al. [19], for different values of m and m_0. In case of Park's model the change in power consumption with change in m_0 values is almost negligible. On the contrary, in case of the proposed model, it is also negligible, but upto $m = 4$. Larger m_0 values consume more power with an increasing rate of power consumption. We also note from Figure 7 that our model consumes less power in comparison, when $m_0 \leq 5$. In addition, from Figure 8 it is more clear that m_0 has negligible effect on power consumption, in case of Park's model. However, we infer from these two figures that to achieve better performance than the Park's model in terms of power consumption, it is better to avoid extremely high values of m_0 (such as $m_0 \geq 7$).

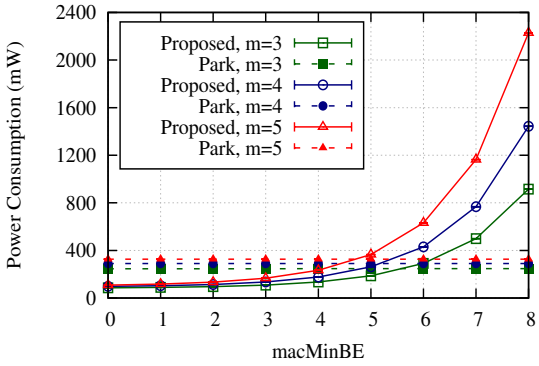

Fig. 7: Power Consumption vs. MAC parameter $macMinBE$ (m_0), for r=3

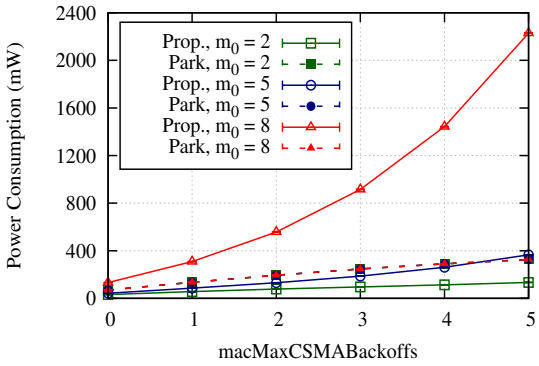

Fig. 8: Power Consumption vs. MAC parameter $macMaxCSMABackoffs$ (m), for r=3

VI. Trade-off between Delay and Power Consumption

In this section, we analyze the trade-off between delay and power consumption of IEEE 802.15.4 MAC. The analysis is done with the help of MATLAB optimization, and toolbox such as curve-fit and fuzzy logic design. At first, we represent the Markov chain-based expressions of average delay (D_{avg}) and average power consumption (P_{avg}), as described in Eqs. 25 and 26, through polynomials of degree seven. Precise approximation of curve-fit can only be achieved by using high degree of polynomial in the curve-fit toolbox, and seven is the maximum limit allowed by the MATLAB curve-fit toolbox while fitting a curve. Another benefit we get from such precise curve-fit is its ability to represent both D_{avg} and P_{avg} as a function of SO, though they belong from different spaces. This helps us to optimize D_{avg} and P_{avg}, with respect to SO. The equivalent expressions of D_{avg} and P_{avg} are as follows:

$$D_{avg} = d_1\, z^7 + d_2\, z^6 + d_3\, z^5 + d_4\, z^4 + d_5\, z^3 + d_6\, z^2 + d_7\, z + d_8 \quad (27)$$

$$P_{avg} = p_1\, z^7 + p_2\, z^6 + p_3\, z^5 + p_4\, z^4 + p_5\, z^3 + p_6\, z^2 + p_7\, z + p_8 \quad (28)$$

where z denotes the value of SO.

It is already observed that the relations of delay and power consumption with SO are contradictory in nature, i.e., longer active periods or higher SO values reduce D_{avg}, but increase P_{avg}. The relations of delay and power consumption with SO are explained in Eqs. 27 and 28, respectively. The average values of associated coefficients are summarized in Table III, along with their ranges corresponding to 95% confidence interval. The representations of D_{avg} and P_{avg} through above equations are irrespective of the degree of polynomials. However, the degree should be same for both the equations, to maintain consistency. We use high degree of polynomials in order to get precise representations equivalent to Eqs. 25 and 26. This conversion from Markov chain-based expressions to corresponding polynomial equations makes it possible to optimize both delay and power consumption with the help of genetic algorithm-based constrained minimization method. We categorize the possible scenarios into four cases, and explain each case with necessary details. Figure 9 represents the constrained optimization of average delay and average power consumption, separately, considering the other as a constraint, as discussed in Case I and Case II. On the other hand, Figure 10 represents the simultaneous constrained optimization of these two performance metrics, as explained in Case III. However, Case I-III are based on a fixed BO value, which is considered as 14 – the maximum possible BO value according to the protocol standard [2]. Therefore, a generalized approach of handling trade-off with variable beacon interval is discussed in Case IV.

TABLE III: The values of the co-efficients corresponding to the 7 degree polynomial curve-fits, when $BO = 14$, $m = 5$, and $m_0 = 2$.

Details of Eq. 27		
Coefficients	**Average**	**Range**
d_1	-0.0003969	(-0.0004902, -0.0003036)
d_2	0.02523	(0.02033, 0.03014)
d_3	-0.6803	(-0.7845, -0.5762)
d_4	10.16	(9.017, 11.3)
d_5	-91.95	(-98.84, -85.05)
d_6	514	(491.7, 536.3)
d_7	-1684	(-1719, -1650)
d_8	2561	(2541, 2580)
Details of Eq. 28		
Coefficients	**Average**	**Range**
p_1	0.00003849	(0.00002943, 0.00004755)
p_2	-0.001594	(-0.002071, -0.001118)
p_3	0.02759	(0.01748, 0.03771)
p_4	-0.2503	(-0.3613, -0.1393)
p_5	1.26	(0.591, 1.93)
p_6	-3.425	(-5.593, -1.257)
p_7	4.524	(1.142, 7.902)
p_8	4.255	(2.39, 6.121)

A. Case I: Optimized average delay with average power consumption as a constraint

This case represents the optimization of average delay for particular upper bounds of average power consumption, and derives the corresponding optimized values of SO_{opt}. We minimize the polynomial expression of D_{avg}, as described in Eq. 27, subject to the constraints: $D_{avg} > 0$ and $P_{avg} \leq$

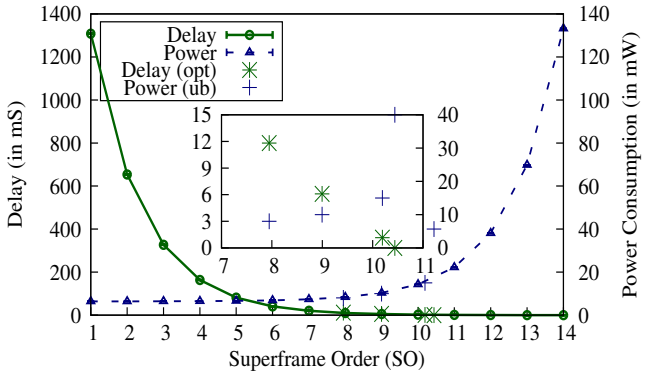

(a) Case I: Optimization of D_{avg}, when power consumption is a constraint

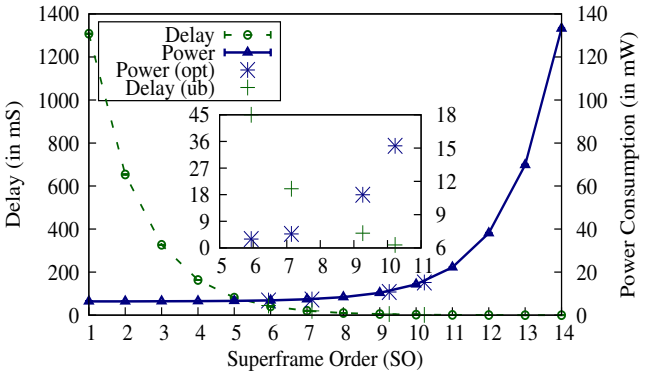

(b) Case II: Optimization of P_{avg}, when delay is a constraint

Fig. 9: Constrained optimization of D_{avg} and P_{avg}, when $BO = 14$, $m = 5$, and $m_0 = 2$

P_{ub}. Therefore, P_{ub} represents the upper bound of allowable power consumption, while minimizing the average delay. We consider different upper bounds for power consumption, and derived the corresponding values of optimized delay (D_{opt}), SO, and SBR, as summarized in Table IV. The optimization process fails to find any D_{opt} in case of very low energy constraint such as $P_{ub} < 7mW$. From 7mW onward we get optimized delays with respect to each power constraint. Table IV contains a detailed account of the optimized values. It is observed that in case of strictly power-constrained scenarios ($7mW \leq P_{ub} \leq 10mW$), very small increase (approximately 1mW) in allowable power consumption values result into steep decrease in D_{opt}, and subsequently, significant increase in SO_{opt} is noted. Whereas, D_{opt} reaches a comparatively stable position with $SO_{opt} \approx 10$, in case of less strict requirements in terms of power consumption. Figure 9(a) depicts few power-constrained QoS requirements and their corresponding optimized values of D_{opt} and SO_{opt}.

B. Case II: Optimized average power consumption with average delay as a constraint

In this case, the optimization of average power consumption is evaluated with respect to particular upper values of average delay. We also derive the corresponding optimized values of SO_{opt}. We minimize the polynomial expression of P_{avg}, as described in Eq. 28, subject to the constraints: $P_{avg} > 0$ and $D_{avg} \leq D_{ub}$. Therefore, D_{ub} represents the upper bound of allowable delay, while minimizing the average power consumption. We consider different upper bounds for delay, and derived the corresponding optimized values of power consumption (P_{opt}), SO, and SBR, as summarized in Table V. Figure 9(b) illustrates few optimized power consumption with respect to different delay constraints. From Table V, it is evident that very high delay constraint (such as $D_{ub} > 500mS$) do not affect the P_{opt} much, and the optimized value reaches a stable value (approximately 6.3741mW) with $S_{opt} \approx 3$. On the other hand, P_{opt} and SO_{opt} decreases rapidly with little increase in D_{ub}, when D_{ub} is low ($D_{ub} < 50mS$), i.e., in case of QoS requirements having strict delay constraints.

Case I and Case II represent optimization of performance metrics with a single objective. Thus, while considering a single objective such as minimizing the average delay we keep the average power consumption as a constraint, and vice versa. However, in practice, a more complex optimization problem is needed to be solved to achieve dynamic trade-off between these two metrics. Thus, we consider Case III as the simultaneous optimization of average delay and average power consumption, while considering constraints for both the metrics.

TABLE IV: Optimized delay and corresponding superframe order with respect to different power consumption constraints, when $BO = 14$, $m = 5$, and $m_0 = 2$

P_{ub} (in mW)	D_{opt} (in mS)	SO_{opt}	SBR
6	NA	NA	NA
7	28.3781	6.6187	0.00599
8	11.8168	7.9460	0.01505
9	8.0297	8.5689	0.02317
10	6.0857	8.9966	0.03117
12	3.6745	9.5950	0.0472
15	1.1508	10.1930	0.07144
25	0.000408	10.4406	0.08482
40	0.000102	10.4406	0.08482
80	0.000087	10.4406	0.08482

TABLE V: Optimized power consumption and corresponding superframe order with respect to different delay constraints, when $BO = 14$, $m = 5$, and $m_0 = 2$

D_{ub} (in mS)	P_{opt} (in mW)	SO_{opt}	SBR
1	15.2061	10.2264	0.07311
2	13.8950	10	0.0625
5	10.7887	9.2625	0.03748
10	8.3736	8.2139	0.01812
20	7.2599	7.1372	0.00859
45	6.8021	5.9421	0.00375
100	6.5904	4.7488	0.00164
225	6.4089	3.5575	0.00071
500	6.3741	2.9678	0.00047
1000	6.3741	2.9636	0.00047

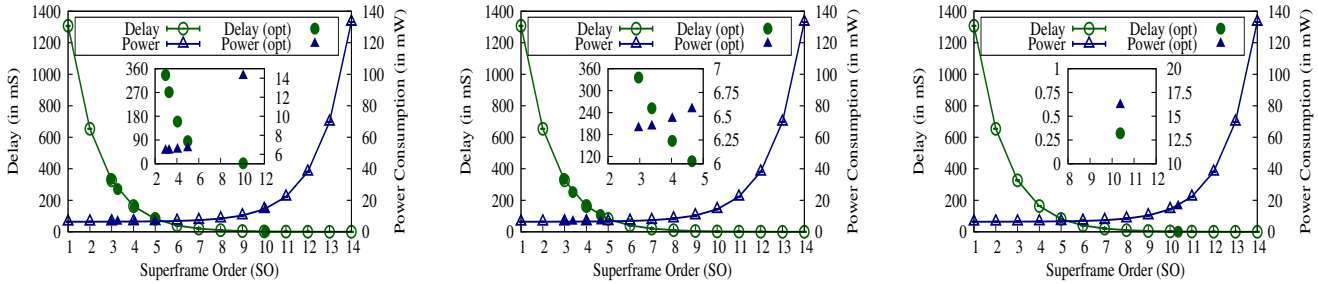

(a) $D_{ub} = 1000mS$ and $P_{ub} = 200mW$ (b) $D_{ub} = 500mS$ and $P_{ub} = 7mW$ (c) $D_{ub} = 5mS$ and $P_{ub} = 100mW$

Fig. 10: Case III: Simultaneous constrained optimization of D_{avg} and P_{avg}, when $BO = 14$, $m = 5$, and $m_0 = 2$

TABLE VI: Simaltaneous constrained optimization of delay and power consumption, when $BO = 14$, $m = 5$, and $m_0 = 2$

D_{ub} (in mS)	P_{ub} (in mW)	D_{opt} (in mS)	P_{opt} (in mW)	SO_{opt}	SBR
1000	200	335.8596	6.3741	2.9636	0.00047
		271.0527	6.3842	3.2748	0.00059
		159.8315	6.4757	4.0504	0.00101
		85.5070	6.6292	4.9827	0.00192
		1.7332	14.2318	10.0616	0.06522
10	8	NA	NA	NA	NA
500	7	335.8803	6.3741	2.9635	0.00047
		251.8657	6.3920	3.3818	0.00063
		162.5446	6.4719	4.0255	0.00099
		107.1459	6.5732	4.6455	0.00152
30	30	NA	NA	NA	NA
5	100	0.3207	16.1706	10.3731	0.08094

C. Case III: Simultaneous constrained optimization of delay and power consumption

The genetic algorithm-based multi-objective constrained optimization allows us to consider more than one constraint during the optimization process. The objective is to optimize both D_{avg} and P_{avg}, as represented in Eqs. 27 and 28, respectively. The multi-objective optimization function is represented as follows:

$$\begin{aligned} & min && D_{avg},\ P_{avg} \\ & \text{subject to} && u_1\ z \leq D_{ub} - u_2 \\ & && v_1\ z \leq P_{ub} - v_2 \end{aligned} \tag{29}$$

By solving this multi-objective optimization function we get the optimal value of z, which represent the SO. For the sake of simplicity we consider linear curve-fits while modeling the constraints for delay and power consumption. The values of the coefficients u_1, u_2, v_1, and v_2 are -63.25, 661.1, 6.133, and -21.49, respectively. These coefficients are used to model the constraints in the form of linear inequalities such as $u_1\ z \leq D_{ub} - u_2$ and $v_1\ z \leq P_{ub} - v_2$. Different pairs of upper bounds, i.e., D_{ub} and P_{ub} are considered while optimizing both D_{avg} and P_{avg}, simultaneously. The resultant values of D_{opt}, P_{opt}, and SO_{opt} are summarized in Table VI.

There are pairs of upper bounds for which we get multiple optimized solutions. Especially, in case of higher upper bounds, i.e., less restriction in the constraints, we get more number of solutions that optimize the multi-objective function depicted in Eq. 29. For example, when the values of D_{ub} and P_{ub} are 1000mS and 200mW, respectively, we get six optimal solutions. Figure 10(a) represents the curves corresponding to D_{avg} and P_{avg}, and points out some of the optimal solutions. In case of high D_{ub} such as 500mS and low P_{ub} such as 7mW, we also get more than one solution, as depicted in Table VI. The solutions are also depicted in Figure 10(b). However, we observe that the reverse, i.e., low D_{ub} and high P_{pb} results into comparatively less number of solutions, as illustrated in Figure 10(c). We may infer that the number of optimal solution depends largely on the delay bound. Thus, a comparatively less restricted delay constraint increases the chances of getting more than one optimal solutions. We also notice that both low D_{ub} and P_{ub} leaves us without any optimized solution. In reality, it represent scenarios having conflicting QoS requirements, such as simultaneous request for low delay and low power consumption.

D. Case IV: Trade-off handling with variable beacon interval

The previous scenarios are based on a fixed BO value, which is considered as 14. Any change in this BO value generates new set of coefficients corresponding to Eqs. 27 and 28, and thus, provides new set of optimized solutions. Moreover, we notice that it is not possible to get any optimized solution in case of conflicting constraints. Therefore, in this particular case we primarily focus on these two issues, and to handle them we introduce a simple fuzzy inference-based solution approach, that derives mathematically justified ratio of SO to BO. It is evident from the definition of SBR that, $SBR = \frac{2^{SO}}{2^{BO}} = 2^{SO-BO}$. Thus, for any particular BO, we are now able to calculate the value of SBR.

The fundamental motivation behind using the concept of fuzzy logic is to avoid linguistic assessment. In assessments based on crisp set theory, network performance metrics (such as delay, power consumption, and throughput) are interpreted as 'low', 'high', and so on, compared to its 'normal' value, which is again dependent on applications. Trade-off solutions that use crisp sets, assume that the definition of 'low' delay is same for more than one applications. However, in real life the scenario is different, and thus, crisp set-based assessment

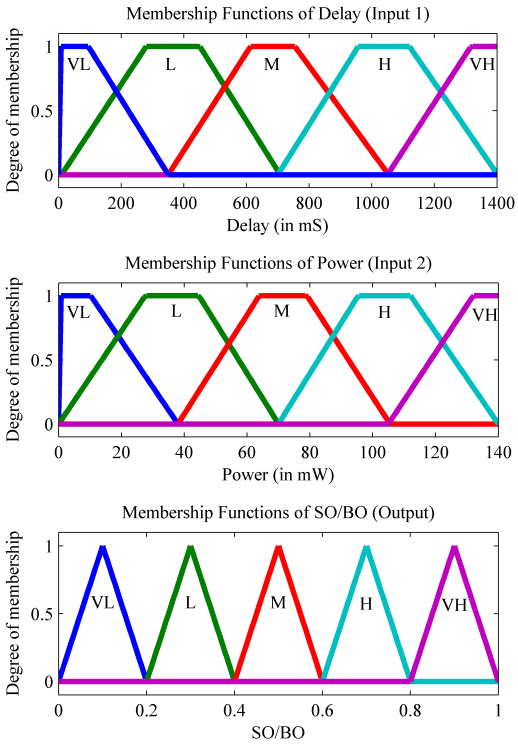

Fig. 11: Membership Functions

TABLE VII: Fuzzy rules considered in our analysis

R. No.	If	Input 1: Delay	and	Input 2: Power	then	Output: $\frac{SO}{BO}$	DC	W
1.	If	VL	and	VH	then	VH	0	1
2.				H		H	1	0.8
3.				M		H	2	0.6
4.				L		M	3	0.4
5.				VL		M	4	0.2
6.		L		VH		VH	1	0.8
7.				H		H	0	1
8.				M		H	1	0.8
9.				L		M	2	0.6
10.				VL		M	3	0.4
11.		M		VH		H	2	0.6
12.				H		H	1	0.8
13.				M		M	0	1
14.				L		L	1	0.8
15.				VL		L	2	0.6
16.		H		VH		M	3	0.4
17.				H		H	2	0.6
18.				M		H	1	0.8
19.				L		L	0	1
20.				VL		H	1	0.8
21.		VH		VH		M	4	0.2
22.				H		M	3	0.4
23.				M		H	2	0.6
24.				L		H	1	0.8
25.				VL		VL	0	1

results into inefficient trade-off solution. In addition to this, contradictory QoS requirement such as simultaneous request for low delay and low energy consumption, is difficult to satisfy through traditional crisp set-based approaches. We already discussed the effectiveness of using SBR to achieve required trade-off, through a Markov chain-based analysis of IEEE 802.15.4 MAC. In this context, we propose a framework based on fuzzy inference system, irrespective of the beacon interval. This system solely depends on the input requirements of delay and energy consumption, and derives the ratio of SO to BO. Brief descriptions of the components such as fuzzy sets, membership functions, and fuzzy rules are provided below.

We consider QoS requirements in terms of delay and power consumption as the two inputs to the fuzzy inference system. The output of the system is a quantified value of $\frac{SO}{BO}$. Five fuzzy sets are considered for each of the input and also for the output. We term them as 'VERY LOW' (VL), 'LOW' (L), 'MODERATE' (M), 'HIGH' (H), and 'VERY HIGH' (VH). Unlike traditional crisp sets, fuzzy inference allows partial membership of a particular input value (delay or power consumption) to these sets depending on the associated membership functions, that are illustrated in Figure 11. The intrinsic components of the system such as the number of fuzzy sets to be considered, the definitions of the membership functions, and the fuzzy rules are user defined. Thus, freedom of application specific modifications are always there.

Popularly used Mamdani model and centroid method are considered in this work as the inference technique and the defuzzification method, respectively. All possible combinations of the input fuzzy sets, i.e., a total of $5 \times 5 = 25$ rules are considered while designing the rule-base. These rules are summarized in Table VII. The fuzzy rules considered in this work are weighted in nature. The weights (W) are derived based on the proposed *degree of contradiction* (DC), associated with each rule. We already discussed about the difficulty of interpreting contradictory QoS requirements. The fuzzy inference-based approach makes it possible to take into consideration the contradictions in requirements by assigning different weights to the fuzzy rules.

Corresponding to the inputs to the fuzzy inference system, we get two input fuzzy sets associated with each fuzzy rule, as also mentioned in Table VII. The input fuzzy sets and their interpretation with respect to the reference frame SO, decide the degree of contradiction for each rule. For example, Rule 1 is associated with input fuzzy sets VL and VH, corresponding to the delay-input and the power consumption-input, respectively, and the output fuzzy set is VH. The conception of this rule is very much obvious from the mutual relation between delay, power consumption and SO. However, in case of Rule 5 the scenario is contradictory as we simultaneously consider 'VL' delay and 'VL' power consumption as input fuzzy sets. Therefore, in this case we not only set the output fuzzy set as 'M', due to the dubious nature of inputs, but also set the weight of the rule as minimum, by considering the degree of contradiction as highest in this case. We consider five degrees of contradictions (0, 1, 2, 3, and 4), five associated weights (0.2, 0.4, 0.6, 0.8, and 1, respectively), and map them with the difference between the logical positions of the input fuzzy sets with reference

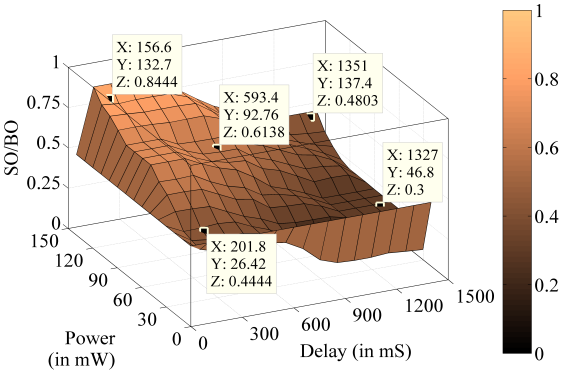

Fig. 12: Result after defuzzification

to the SO as the independent axis. Thus, whenever the QoS requirements in terms of delay and power consumption are contradictory in nature, the corresponding fuzzy rules are fired with less weights, depending on the degree of contradiction. Based on the above mentioned membership functions and rules, we finally achieve the quantification of $\frac{SO}{BO}$, within the range of 0 to 1. For each pair of delay and power consumption input we get a quantified output, which if multiplied with the then BO generates the necessary SO. Figure 12 illustrates the final result of defuzzification process. This figure contains the set of quantified $\frac{SO}{BO}$ values corresponding to each possible pair of delay and power consumption.

VII. Conclusion

In this work, we proposed a Markov chain-based analysis of slotted CSMA/CA algorithm of ZigBee protocol, with considering backoff freezing and ACK timeout. We primarily focus on two MAC PIB attributes – BO and SO, and consequently introduce a variable SBR for adaptive tuning to achieve a trade-off between delay and power consumption. The results obtained from our work, yield 35% less delay, on an average, compared to one of the existing works. The results also prove that the proposed model consumes reduced power, especially when the contention window size is within a medium range. Moreover, constrained optimization of delay and power consumption results into optimal values of SO, for a constant BI. The fuzzy inference-based approach further provides trade-off solution for dynamic BIs. We show that by proper tuning of BO and SO, it is possible to achieve an SBR value, which triggers a trade-off between D_{avg} and P_{avg}. In the future, we wish to extend this work for unsaturated network, by considering explicit traffic models. Moreover, we also plan to tune these important MAC PIB attributes, while optimizing QoS attributes, such as reliability.

References

[1] J. Zheng and M. Lee, "Will IEEE 802.15.4 make ubiquitous networking a reality?: A discussion on a potential low power, low bit rate standard," *IEEE Comm. Magazine*, vol. 42, no. 6, pp. 140–146, June 2004.

[2] *IEEE Standard for Local and metropolitan area networks - Part 15.4: Low-Rate Wireless Personal AreaNetworks (LR-WPANs) - Amendment 6: TV White Space Between 54 MHz and 862 MHz Physical Layer*, Std., April 2014.

[3] J. Hespanha, P. Naghshtabrizi, and Y. Xu, "A Survey of Recent Results in Networked Control Systems," *Proceedings of the IEEE*, vol. 95, no. 1, pp. 138–162, Jan 2007.

[4] G. Lu, B. Krishnamachari, and C. Raghavendra, "Performance evaluation of the IEEE 802.15.4 MAC for low-rate low-power wireless networks," in *IEEE ICPCC*, 2004, pp. 701–706.

[5] B. Bougard, F. Catthoor, D. Daly, A. Chandrakasan, and W. Dehaene, "Energy efficiency of the IEEE 802.15.4 standard in dense wireless microsensor networks: modeling and improvement perspectives," in *Proceedings of Design, Automation and Test in Europe*, March 2005, pp. 196–201 Vol. 1.

[6] A. Koubaa, M. Alves, and E. Tovar, "A comprehensive simulation study of slotted CSMA/CA for IEEE 802.15.4 wireless sensor networks," in *IEEE IWFCS*, Torino, Italy, 2006, pp. 183 – 192.

[7] J. Zheng and M. J. Lee, "A Comprehensive Performance Study of IEEE 802.15.4," *Sensor Network Operations*, pp. 218–237, 2006.

[8] G. Bianchi, "Performance analysis of the IEEE 802.11 distributed coordination function," *IEEE Journal on Selected Areas in Communications*, vol. 18, pp. 535–547, March 2000.

[9] J. Misic, V. Misic, and S. Shafi, "Performance of IEEE 802.15.4 beacon enabled PAN with uplink transmissions in non-saturation mode - access delay for finite buffers," in *First International Conference on Broadband Networks*, Oct 2004, pp. 416–425.

[10] J. Misic, S. Shafi, and V. Misic, "Performance of a beacon enabled IEEE 802.15.4 cluster with downlink and uplink traffic," *IEEE Trans. on Parallel and Distr. Systems*, vol. 17, no. 4, pp. 361–376, April 2006.

[11] X. Ling, Y. Cheng, J. Mark, and X. Shen, "A Renewal Theory Based Analytical Model for the Contention Access Period of IEEE 802.15.4 MAC," *IEEE Transaction on Wireless Communication.*, vol. 7, no. 6, pp. 2340–2349, June 2008.

[12] P. K. Sahoo and J.-P. Sheu, "Modeling IEEE 802.15.4 based wireless sensor network with packet retry limits," in *PE-WASUN*, 2008, pp. 63–70.

[13] S. Pollin, M. Ergen, S. Ergen, B. Bougard, L. D. Perre, I. Moerman, A. Bahai, P. Varaiya, and F. Catthoor, "Performance Analysis of Slotted Carrier Sense IEEE 802.15.4 Medium Access Layer," *IEEE Transactions on Wireless Communications*, vol. 7, pp. 3359 – 3371, September 2008.

[14] C. Jung, H. Hwang, D. K. Sung, and G. Hwang, "Enhanced Markov Chain Model and Throughput Analysis of the Slotted CSMA/CA for IEEE 802.15.4 Under Unsaturated Traffic Conditions," *IEEE Transactions on Vehicular Technology*, vol. 58, no. 1, pp. 473–478, Jan 2009.

[15] C. Buratti, "Performance Analysis of IEEE 802.15.4 Beacon-Enabled Mode," *IEEE Transactions on Vehicular Technology*, vol. 59, no. 4, pp. 2031–2045, May 2010.

[16] A. Faridi, M. Palattella, A. Lozano, M. Dohler, G. Boggia, L. Grieco, and P. Camarda, "Comprehensive Evaluation of the IEEE 802.15.4 MAC Layer Performance With Retransmissions," *IEEE Transactions on Vehicular Technology*, vol. 59, no. 8, pp. 3917–3932, Oct 2010.

[17] J. Misic, S. Shafi, and V. Misic, "Maintaining reliability through activity management in 802.15.4 sensor networks," in *Second International Conference on Quality of Service in Heterogeneous Wired/Wireless Networks*, Lake Vista, FL, Aug 2005, pp. 10 pp.–5.

[18] P. Park, C. Fischione, and K. H. Johansson, "Adaptive IEEE 802.15.4 Protocol for Energy Efficient, Reliable and Timely Communications," in *IPSN*, Stockholm, Sweden, April 2010, pp. 327–338.

[19] P. Park, P. Di Marco, C. Fischione, and K. Johansson, "Modeling and Optimization of the IEEE 802.15.4 Protocol for Reliable and Timely Communications," *IEEE Transactions on Parallel and Distributed Systems*, vol. 24, no. 3, pp. 550–564, March 2013.

[20] S. Moulik, S. Misra, and D. Das, "AT-MAC: Adaptive MAC-frame Payload Tuning for Reliable Communication in Wireless Body Area Networks," *IEEE Transactions on Mobile Computing*, vol. PP, no. 99, pp. 1–1, 2016.

[21] O. Stecklina, S. Kornemann, and M. Methfessel, "A secure wake-up scheme for low power wireless sensor nodes," in *Collaboration Technologies and Systems (CTS), 2014 International Conference on*, May 2014, pp. 279–286.

[22] A. Farhad, Y. Zia, S. Farid, and F. B. Hussain, "A traffic aware dynamic super-frame adaptation algorithm for the IEEE 802.15.4 based networks," in *Wireless and Mobile (APWiMob), 2015 IEEE Asia Pacific Conference on*, Aug 2015, pp. 261–266.

[23] A. Farhad, S. Farid, Y. Zia, and F. B. Hussain, "A delay mitigation dynamic scheduling algorithm for the IEEE 802.15.4 based WPANs," in *2016 International Conference on Industrial Informatics and Computer Systems (CIICS)*, March 2016, pp. 1–5.